

Surprises in the Phase Diagram of an Anderson Impurity Model for a Single C_{60}^{n-} Molecule

Lorenzo De Leo¹ and Michele Fabrizio^{2,3}

¹*Department of Physics and Center for Material Theory, Rutgers University, Piscataway, New Jersey 08854, USA*

²*International School for Advanced Studies (SISSA), Via Beirut 2-4, I-34014 Trieste, Italy*

³*The Abdus Salam International Center for Theoretical Physics (ICTP), P.O. Box 586, I-34014 Trieste, Italy*

(Received 10 January 2005; published 17 June 2005)

We find by Wilson numerical renormalization group and conformal field theory that a three-orbital Anderson impurity model for a C_{60}^{n-} molecule has a very rich phase diagram which includes non-Fermi-liquid stable and unstable fixed points with interesting properties, most notably high sensitivity to doping n . We discuss the implications of our results to the conductance behavior of C_{60} -based single-molecule transistor devices.

DOI: 10.1103/PhysRevLett.94.236401

PACS numbers: 71.10.Hf, 72.15.Qm, 73.63.-b

The characteristic behavior of an Anderson impurity model (AIM) emerges often unexpectedly in physical contexts which are apparently far away from magnetic alloys. The typical example is the conductance behavior of nano-scale devices, e.g., quantum dots and single-molecule transistors (SMT), where Kondo-assisted tunneling may lead to nearly perfect transmission at zero bias in spite of a large charging energy [1]. Usually the two conduction leads are bridged by a single quantum dot or molecular level, which therefore behaves effectively as a one-orbital AIM. Less common is the case when several levels happen to be nearby degenerate, thus realizing in practice a multi-orbital AIM. This may be achieved, for instance, in SMTs built with high-symmetry molecules. Recently, a zero-bias anomaly has been reported for a C_{60} based SMT [2], which has been proven to be of the Kondo-type by its splitting under the action of a magnetic field or magnetic leads [3]. Fullerene's large electron affinity is known to yield to electron transfer into C_{60} when adsorbed on metallic substrates. The actual number of doped electrons depends on the substrate [4], but may also be controlled by attaching alkali atoms to the molecule [5]. In this case a variety of conductance behavior has been reported depending on the number of K atoms attached to C_{60} [5], ranging from Kondo-like resonances to Fano-like antiresonances.

Motivated by this opportunity, in this Letter we study the behavior of an AIM for C_{60}^{n-} by Wilson numerical renormalization group (NRG) [6] and conformal field theory (CFT) [7]. We obtain a phase diagram that includes Fermi- and non-Fermi-liquid phases, with a doping dependence qualitatively in agreement with experiments. In particular, we find a Kondo-like zero-bias anomaly for doping $n = 1$, likely the case of C_{60} on Au [4], as found in Refs. [2,3]. For $n = 2$, which should correspond to pure or slightly K -doped C_{60} on Ag [4], we predict instead a conductance minimum at zero bias, compatible with actual observations [5]. Finally, for $n = 3$ we find a conductance minimum with a nonanalytic voltage behavior $G(V) - G(0) \sim |V|^{2/5}$.

The lowest unoccupied molecular orbitals of C_{60} are threefold degenerate t_{1u} orbitals [8]. The electron-electron

interaction acts as if these orbitals were effectively p orbitals. Therefore the Coulomb energy of a C_{60}^{n-} molecule with n valence electrons into a configuration with total spin S and angular momentum L is $\mathcal{H}_{\text{int}} = \mathcal{H}_U + \mathcal{H}_J$, with $\mathcal{H}_U = U(n - n_0)^2/2$ and $\mathcal{H}_J = -J[2S(S + 1) + \frac{1}{2}L(L + 1)]$. The reference valency, n_0 , is controlled in SMTs by the gate voltage, the metal substrate, and the alkali doping. The Coulomb exchange, $J > 0$, favoring high-degeneracy states (conventional Hund's rules), competes in C_{60} with the Jahn-Teller coupling to eight fivefold-degenerate vibrational modes of H_g symmetry [8], which, on the contrary, prefers low-degeneracy configurations (inverted Hund's rules). If the vibrational frequencies, ranging from 35 to 196 meV [8], are larger than the Kondo temperature, one can neglect retardation effects, which amount to renormalize $J \rightarrow J - 3E_{\text{JT}}/4$, where $E_{\text{JT}} \approx 169$ meV is the Jahn-Teller energy gain. Although first principle calculations [9] do predict an inverted effective exchange $J - 3E_{\text{JT}}/4 \approx -50$ meV, in what follows we consider both $J > 0$ and $J < 0$ cases.

The impurity is coupled to a bath of conduction electrons, and both the bath and the hybridization are, for simplicity, assumed to be $SU(6)$ and particle-hole (p - h) invariant. When discussing the stability of the fixed points, we shall take into account deviations from this high-symmetry case. The noninteracting Hamiltonian, $\mathcal{H}_0 = \mathcal{H}_{\text{bath}} + \mathcal{H}_{\text{hyb}}$ can always be written as a one-dimensional chain of noninteracting electrons, $\mathcal{H}_{\text{bath}} = \sum_{\sigma m} \sum_{i \geq 1} t_i (c_{i m \sigma}^\dagger \times c_{i+1 m \sigma} + \text{H.c.})$, hybridized at one edge to the impurity, $\mathcal{H}_{\text{hyb}} = V \sum_{\sigma m} (d_{m \sigma}^\dagger c_{1 m \sigma} + \text{H.c.})$. Here $c_{i m \sigma}^\dagger$ and $c_{i m \sigma}$ are, respectively, the creation and annihilation conduction-electron operators at chain site i with spin $\sigma = \uparrow, \downarrow$ and angular momentum component $m = -1, 0, 1$, while $d_{m \sigma}^\dagger$ and $d_{m \sigma}$ are the analogous impurity operators.

Although we analyzed by NRG the full AIM, $\mathcal{H}_{\text{AIM}} = \mathcal{H}_0 + \mathcal{H}_{\text{int}}$, the CFT analysis is more conveniently done for the Kondo model onto which the AIM maps for large U . One finds that $\mathcal{H}_{\text{AIM}} \rightarrow \mathcal{H}_{\text{bath}} + \mathcal{H}_J + \mathcal{H}_K$, where the Kondo exchange is given by

$$\mathcal{H}_K = \frac{4V^2}{U} \sum_{l,\lambda,s,\sigma} \{c_1^\dagger \otimes c_1\}_{l\lambda,s\sigma} \{d^\dagger \otimes d\}_{l\lambda,s\sigma}^\dagger \quad (1)$$

$\{d^\dagger \otimes d\}_{l\lambda,s\sigma} = \sum C_{1m1-m'}^{l\lambda} (-1)^{m'-1} C_{1/2\alpha 1/2-\alpha'}^{s\sigma} (-1)^{\alpha'-1/2} \times (d_{m\alpha}^\dagger d_{m'\alpha'} - 1/2 \delta_{mm'} \delta_{\alpha\alpha'})$ is the impurity p - h operator with angular momentum $l = 0, 1, 2$, and z component λ , as well as spin $s = 0, 1$, and z component σ , and analogously for the operator at site 1 of the chain. $C_{ijzj'z'}^{JJ_z}$ are Clebsch-Jordan coefficients. Notice that $\{d^\dagger \otimes d\}_{00,00} = (n_0 - 3)/\sqrt{6}$ is zero when $n_0 = 3$. Since the $U(6)$ symmetry of $\mathcal{H}_{\text{bath}}$ is reduced to charge $U(1)$, spin $SU(2)$, and orbital $O(3)$, the proper conformal embedding of the conduction electrons is $U(6)_1 \supset U(1) \times SU(2)_3 \times SU(2)_8 \times Z_3$, where $SU(2)_3$ refers to spin and $SU(2)_8$ to the angular momentum [10]. The 3-state Potts sector Z_3 , which reflects orbital permutational symmetry, can be interpreted as emerging out of the charge isospin $SU(2)_3 \supset U(1) \times Z_3$, [7] with generators $I_z = \sum_i (n_i - 3)/2$, $I^+ = \sum_i (-1)^i \times \sum_{m=-1}^1 (-1)^m c_{im}^\dagger c_{i-m}^\dagger$, and $I^- = (I^+)^\dagger$. They commute with $\mathcal{H}_{\text{bath}}$ and also with the Kondo-exchange terms with $(l, s) = (1, 0), (0, 1), (2, 1)$, while they do not with those having $(l, s) = (0, 0), (2, 0), (1, 1)$. We recall that the Z_3 Potts model has primary fields I, σ, Z , and ϵ , with dimensions 0, 1/15, 2/3, and 2/5, respectively [7].

Since the AIM is invariant upon $n_0 \rightarrow 6 - n_0$, we need to consider only $n_0 = 1, 2, 3$. For $n_0 = 1$, \mathcal{H}_J is ineffective, leading at large U to a conventional Kondo-screened $SU(6)$ model. Conversely, nontrivial behavior may appear for $n_0 = 2, 3$. Here the Kondo screening, controlled by the Kondo temperature T_K , is hampered by the exchange splitting J . While the former takes advantage of the impurity coherently tunneling among all available n_0 -electron configurations, the latter tends to lock the impurity into a subset of states with well defined S and L . When $|J| \sim T_K$, neither prevails and a nontrivial behavior may emerge.

In the p - h symmetric case, $n_0 = 3$, the available impurity states have quantum numbers $(S, L) = (3/2, 0), (1/2, 2), (1/2, 1)$. For conventional Hund's rules, $J > 0$, the lowest energy state has $(S, L) = (3/2, 0)$, while for $J < 0$ $(S, L) = (1/2, 1)$ is favored. Let us first assume a positive and very large $J \gg T_K$. In this case the impurity effectively behaves as a spin-3/2. If we project (1) onto the above impurity configuration, only $(l, s) = (0, 1)$ survives, which is just the spin exchange $(8V^2/3U) \mathbf{S} \cdot \mathbf{S}_1$. The model reduces to a spin-3/2 impurity coupled to three conduction channels; hence it describes a perfectly Kondo-screened fixed point which has Fermi-liquid (FL) behavior. The impurity density of states (DOS), $\rho(\epsilon)$, is unaffected by \mathcal{H}_{int} at the chemical potential, $\rho(0) = \rho_0$, meaning a perfect transmission in the SMT, $G/(2e^2/h) = \rho(0)/\rho_0 = 1$, with G the zero-bias conductance per orbital.

In the opposite extreme of a strong inverted Hund's rule, $J \ll -T_K < 0$, the impurity locks into the $(S, L) = (1/2, 1)$ state. The Kondo exchange projected onto this subspace contains $(l, s) = (1, 0), (0, 1), (2, 1)$, hence still commutes

with the isospin generators. Thus we expect the asymptotic spectrum to be described by conformal towers identified by the quantum numbers of the isospin, I , spin, S , and angular momentum, L . To infer the fixed point, let us assume a Kondo exchange $J_K \sim V^2/U$ much larger than the bath bandwidth. In this case we have first to solve the two-site problem which includes the impurity and site 1 of the chain. The lowest energy states are obtained by coupling into an overall singlet the impurity with a $(S, L) = (1/2, 1)$ electron configuration. Yet one can form three states at site 1 with $(S, L) = (1/2, 1)$, namely, through 1, 3, or 5 electrons. The net result is that the two-site ground state is threefold degenerate and represents an effective isospin-1 impurity. Projecting onto this manifold the hopping term connecting site 1 to site 2, we get a new Kondo exchange acting only among isospins, namely, $\propto (t_1^2/J_K) \mathbf{I} \cdot \mathbf{I}_2$. This model describes an isospin-1 three-channel Kondo model which is non-Fermi liquid (NFL). By applying the fusion hypothesis [11], which is a formal way in CFT to make the impurity dissolve, with its quantum numbers, into the conduction sea, we argue that the fixed point is obtained by fusing the $\pi/2$ phase-shifted chain with an iso-spin-1 primary field. The spectrum obtained in this way agrees with the actual NRG results; see Table I [12]. The approach to the fixed point is controlled by the leading irrelevant operator of dimension 7/5, which is the first descendant of the iso-spin-1 primary field [11] and represents the residual, actually attractive, interaction among the conduction electrons once the impurity has been absorbed. This operator leads to a singular local isospin susceptibility, $\chi_I \sim T^{-1/5}$, whose components are the compressibility and the pairing susceptibility in the $S = L = 0$ Cooper channel. The fixed point has a residual entropy $S(0) = 1/2 \times \ln[(\sqrt{5} + 1)/(\sqrt{5} - 1)]$ and an impurity DOS $\rho(0) = \rho_0/(1 + \sqrt{5})$, with $\rho(\epsilon) - \rho(0) \sim |\epsilon|^{2/5}$ [13]. This implies that the tunneling conductance approaches a fractional value at zero temperature, $G(T=0)/(2e^2/h) = 1/(1 + \sqrt{5})$, in a power-law fashion, $G(T) - G(0) \sim T^{2/5}$. The fixed point is, however, unstable towards symmetry-breaking boundary terms which correspond in Table I to physical operators with dimensions smaller than 1. They include p - h and gauge symmetry breaking in the $S = L = 0$ Cooper channel, i.e., the $(I, S, L) = (1, 0, 0)$ operator, as well as quadrupolar distortions and spin-orbit coupling, the $(I, S, L) = (0, 0, 2)$ and $(0, 1, 1)$ operators, respectively.

Since the two stable fixed points for $J \ll -T_K$ and $J \gg T_K$ are essentially different, we expect an unstable fixed point in between, which we actually find by NRG for a $J_* \sim -T_K$. The NRG spectrum shows that the isospin symmetry is not restored at this point, unlike at the two stable ones, which forces us to deal with independent charge $U(1)$ and Potts Z_3 sectors. The conformally invariant boundary conditions of a 3-state Potts model in two dimensions are well characterized [14] and include stable *fixed* boundary conditions, only one of the 3 states is allowed at the boundary, less stable *mixed* boundary con-

TABLE I. Left part: low-energy spectrum at the non-Fermi-liquid stable fixed point for $n_0 = 3$, in units of the fundamental level spacing, as predicted by CFT, E_{CFT} , and as obtained by NRG, E_{NRG} . Right part: dimension x of the most relevant boundary operators.

I	S	L	E_{CFT}	E_{NRG}	I	S	L	x
1/2	0	0	0	0	0	0	0	0
0	1/2	1	1/5	0.199	1	0	0	2/5
1	1/2	1	3/5	0.603	1/2	1/2	1	1/2
1/2	0	2	3/5	0.599	0	0	2	3/5
1/2	1	1	3/5	0.599	0	1	1	3/5

ditions, two states are allowed, and lastly an unstable *free* boundary condition. We observe that the Kondo-screened phase and the non-Fermi-liquid one can be identified, respectively, as the *fixed* and *mixed* boundary conditions in the Potts sector. Indeed, the non-Fermi-liquid fixed-point spectrum can also be obtained fusing the Kondo-screened fixed point with the Z_3 primary field ϵ , in agreement with the boundary CFT of the 3-state Potts model [14]. The unstable fixed point should then correspond to the *free* boundary condition. It has been shown [14] that a proper description of the *free* boundary condition in the 3-state Potts model requires a larger set of conformal towers which include the so-called C -disorder fields [15] of dimensions $1/40$, $1/8$, $21/40$, and $13/8$. We actually find that the unstable fixed point is simply obtained by the Kondo-screened one upon fusion with the same $1/8$ primary field that allows one to turn the fixed into free boundary conditions in the 3-state Potts model [14]; see Table II. From the right panel in Table II it turns out that the operator which moves away from the fixed point has quantum numbers $(Q, S, L, Z_3) = (0, 0, 0, Z)$ and dimension $2/3$. This implies that the effective energy scale which controls the deviation from the unstable point behaves as $T_- \sim |J - J_*|^3$. The most relevant symmetry-breaking operator has quantum numbers $(Q, S, L, Z_3) = (2, 0, 0, I)$ and corresponds to the $S = L = 0$ Cooper channel. The corresponding pairing susceptibility diverges at zero temperature $\chi_{SC} \sim T^{-1/3}$. The next relevant operators of dimension $2/3$ are the same quadrupolar distortions and spin-orbit coupling as for the stable non-Fermi-liquid fixed point. The residual entropy is $S(0) = 1/2 \ln 3$ and the impurity DOS $\rho(0) = \rho_0/2$ with $\rho(\epsilon) - \rho(0) \sim -\epsilon^2$, implying a tunneling conductance $G(0)/(2e^2/h) = 1/2$.

Unlike the stable NFL fixed point, the unstable one survives p - h symmetry breaking. Therefore, although both regimes with $J \ll -T_K$ and $J \gg T_K$ should have Fermi-liquid behavior away from p - h symmetry, an unstable NFL fixed point is still expected to intrude between them. The NRG analysis confirms this CFT prediction not only slightly but also far away from p - h symmetry. For instance, we still observe an unstable fixed point for $J_* \sim -T_K$ when the average impurity occupancy $n_0 = 2$. In this case for $J \ll -T_K$ the impurity locks into a total singlet,

TABLE II. Same as Table I for the unstable fixed point. This time, however, the states and operators are labeled by (Q, S, L, Z_3) where Q refers to the $U(1)$ charge sector and Z_3 to the Potts sector.

Q	S	L	Z_3	E_{CFT}	E_{NRG}	Q	S	L	Z_3	x
1	0	0	1/8	0	0	0	0	0	I	0
0	1/2	1	1/40	1/6	0.162	2	0	0	I	1/3
1	0	2	1/40	1/2	0.488	1	1/2	1	σ	1/2
1	1	1	1/40	1/2	0.489	0	0	0	Z	2/3
2	1/2	1	1/40	1/2	0.491	0	0	2	σ	2/3
0	1/2	1	21/40	2/3	0.675	0	1	1	σ	2/3
0	1/2	2	1/8	2/3	0.643	1	1/2	1	ϵ	5/6
0	3/2	0	1/8	2/3	0.644					
3	0	0	1/8	2/3	0.648					

$S = L = 0$, which decouples from the conduction sea. For $J \gg T_K$ the impurity instead is in a state with $S = L = 1$ which, due to the $(l, s) = (0, 0)$ term in Eq. (1), gets fully screened by four conduction electrons. These two phases turn out to be still separated by a critical point, which we find can be obtained by fusing the spectrum of the unscreened fixed point ($J \ll -T_K$) with the dimension- $1/8$ primary field of the extended Z_3 sector. The operator content at this unstable fixed point is exactly the same as in the case of $n_0 = 3$, thus showing that they are connected by a whole critical line $J_*(n_0)$. We find that $J_* \sim -T_K$ for $n_0 \in [2, 3]$. For $n_0 < 2$, $|J_*|$ increases and merges into a mixed-valence critical point $J_* \sim -U$ for $n_0 \rightarrow 1$, as sketched qualitatively in Fig. 1.

Let us discuss now the behavior of the impurity DOS in the various phases, which is directly proportional to the SMT conductance. In Fig. 2 we draw the DOS across the unstable NFL fixed point for $n_0 = 3$. We notice that the DOS displays two distinct features at low energy. There is a broad resonance which is smooth across the transition. On top of that, there is a narrow peak in the Kondo-screened phase which shrinks, disappears at the fixed point, and transforms in a narrow cusplike pseudogap within the NFL phase. We argue [16] that this dynamical behavior

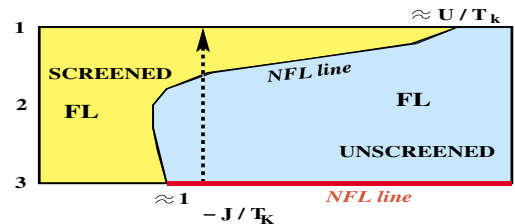


FIG. 1 (color online). Qualitative phase diagram of the AIM as a function of n_0 and $-J/T_K$ for $J < 0$. Both screened and unscreened regions are Fermi liquids (FL). Screened or unscreened refers to the presence or absence of a Kondo resonance in the DOS. The critical line separating them is non-Fermi liquid (NFL), as well as the line at $n_0 = 3$ for $-J/T_K$ above the critical value ≈ 1 . The arrow indicates the path along which the DOS in the right panel of Fig. 3 is calculated.

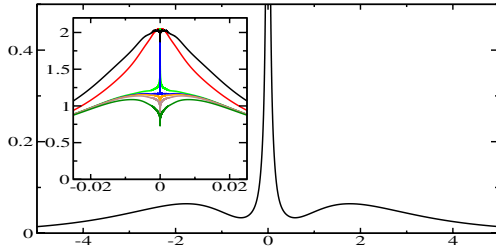


FIG. 2 (color online). NRG impurity DOS at $n_0 = 3$ with $U = 2$ and $\rho_0 = 2$ in units of half the bath bandwidth [12]. The large figure shows the DOS on a large scale at $J = 0$, where the Hubbard sidebands and the Kondo resonance are both visible. In the inset we show the low-energy part across the unstable fixed point. The curves from the top one downwards correspond to $J = 0.0, -0.01, -0.017, -0.018, -0.02, -0.035, -0.043$.

is controlled by two energy scales. One is the aforementioned scale that measures the deviation from the fixed point, $T_- \sim |J - J_*|^3$, and sets the magnitude of the narrow resonance as well as of the pseudogap, $\rho(\epsilon) - \rho(0) \sim \rho(0)|\epsilon/T_-|^{2/5}$. The other is a high energy scale, $T_+ \sim |J_*|$, which sets the width of the broad resonance.

Since it is unlikely that experimentally the system finds itself near the unstable fixed point, in Fig. 3 we draw the low-energy part of the DOS with $n_0 = 1, 2, 3$ far away from the unstable fixed point. In the figure we show the two cases: 3(a) $J = 0$, standard Kondo effect; 3(b) $J < 0$ along a path like the one drawn in Fig. 1. Unlike the $J = 0$ case (also representative of all positive J 's), for $J < 0$ the DOS turns out to be highly sensitive to the doping n_0 , similar to what is observed experimentally [5].

We end by discussing the role of quadrupolar distortions which lower the icosahedral symmetry of isolated C_{60} and presumably exist in real SMT devices. In their presence the unstable fixed-point critical region is replaced by a crossover region, more or less smooth depending on the value of the distortion. Yet the spectral properties inside the inverted Hund's rule region should still differ from a conventional perfectly screened Kondo-like behavior, particularly when the sensitivity to the doping is concerned.

In conclusion, we have shown that a realistic Anderson impurity model of a C_{60}^{n-} molecule displays a phase diagram which includes non-Fermi-liquid phases and critical

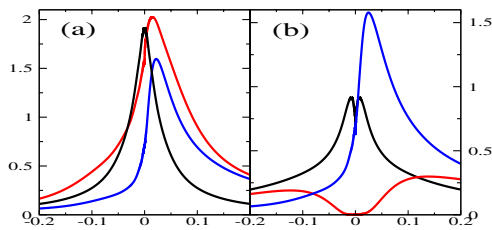


FIG. 3 (color online). Low-energy impurity DOS at $n_0 = 1, 2, 3$. (a) $J = 0$. The peaks of the curves with decreasing $n_0 = 3, 2, 1$ gradually move towards positive energies. (b) $J = -0.075$. $n_0 = 3$ is the curve with the cusp at the chemical potential, $n_0 = 2$ that with the large pseudogap, and $n_0 = 1$ the other one.

points with anomalous properties, most notably higher sensitivity to doping n and quadrupolar distortions than to magnetic field, especially for $n > 1$. These results indicate a possibly very interesting behavior of C_{60} based SMTs. Provided C_{60} could be endowed with more than one electron in a controllable way, e.g., adsorbed on proper metal substrates [4] or by alkali doping [5], fractional zero-bias anomalies with power-law temperature-voltage behavior might eventually show up. Moreover, the enhancement of the pairing fluctuations that emerges out of our analysis suggests an anomalous behavior when superconducting leads are used, as, for instance, an increase of the zero-bias anomaly below the lead critical temperature if much smaller than T_K .

In view of recent speculations about the role of unstable fixed points in single AIM's in the context of strongly correlated models on large-coordination lattices [17], our results may also have important implications for alkali-doped fullerenes. We will return to this in a later work.

We acknowledge very helpful discussions with A. O. Gogolin, I. Affleck, and E. Tosatti. This work has been partly supported by MIUR COFIN2004, FIRBRBAU017S8R, and FIRBRBAU01LX5H.

- [1] T. Ng and P. Lee, Phys. Rev. Lett. **61**, 1768 (1988); L. Glazman and M. Raikh, JETP Lett. **47**, 452 (1988).
- [2] L. H. Yu and D. Natelson, Nano Lett. **4**, 79 (2004).
- [3] A. N. Pasupathy *et al.*, Science **306**, 86 (2004).
- [4] S. Modesti, S. Cerasari, and P. Rudolf, Phys. Rev. Lett. **71**, 2469 (1993); C. Cepek *et al.*, Surf. Sci. **454-456**, 467 (2000).
- [5] R. Yamachika *et al.*, Science **304**, 281 (2004).
- [6] H. R. Krishnamurthy, J. W. Wilkins, and K. G. Wilson, Phys. Rev. B **21**, 1003 (1980); **21**, 1044 (1980).
- [7] P. Di Francesco, P. Mathieu, and D. Sénéchal, *Conformal Field Theory* (Springer, New York, 1996).
- [8] See O. Gunnarsson, Rev. Mod. Phys. **69**, 575 (1997), and references therein.
- [9] M. Luders *et al.*, Philos. Mag. B **82**, 1611 (2002).
- [10] The subscript k of $SU(2)_k$ denotes the level of the Kac-Moody algebra [7], and, roughly speaking, counts the number of channels used to build up the *spin* operators as well as their intrinsic *spin* (1/2 for the true spin and 1 for the angular momentum).
- [11] I. Affleck and A. W. W. Ludwig, Nucl. Phys. **B360**, 641 (1991).
- [12] The NRG calculations have been performed with $\Lambda = 3$ [6] and keeping up to 4500 states per iteration. We implemented the charge $U(1)$, spin $SU(2)$ and orbital $O(3)$ symmetries.
- [13] I. Affleck and A. W. W. Ludwig, Phys. Rev. B **48**, 7297 (1993); Phys. Rev. Lett. **67**, 161 (1991).
- [14] I. Affleck, M. Oshikawa, and H. Saleur, J. Phys. A **31**, 5827 (1998).
- [15] A. B. Zamolodchikov and V. A. Fateev, Zh. Eksp. Teor. Fiz. **90**, 1553 (1986) [Sov. Phys. JETP **63**, 913 (1986)].
- [16] L. De Leo and M. Fabrizio, Phys. Rev. B **69**, 245114 (2004).
- [17] M. Fabrizio *et al.*, Phys. Rev. Lett. **91**, 246402 (2003).